

Ground Targets Recognition from Flying Vehicles using Camera/SAR Imaging Systems

Alaa El-Din Sayed Hafez, Wiedo Hu, and Ahmed Mohamed Gharyb

Abstract— This paper proposes a ground targets recognition system for flying vehicles using Camera/Synthetic Aperture Radar (SAR) imaging systems. The proposed method is an image processing technique to improve the precision of the INS for detecting and tracking the ground objects from flying vehicles. Template matching is one of the methods used for ground object detection and tracking. Synthetic Aperture Radar (SAR) is also used as ground object detection with ATR technique. Robust and reliable object detection is a critical step of object recognition. Our focus is on flying systems equipped with camera and SAR to capture photos for the ground and recognize it. SAR is a type of imaging radar in which the relative movement of the antenna with respect to the target is utilized. Through the simultaneous processing of the radar reflections over the movement of the antenna via the Range Doppler Algorithm (RDA). The proposed method is independent on the altitude or the orientation of the object. The algorithm is simulated using Matlab program and the numerical experiments are shown which verify the object detection for a wide range altitude and orientation. The results show superiority of this method for identifying and recognizing the ground objects.

Index Terms—INS, Template Match, SAR, ATR

I. INTRODUCTION

An INS is a navigation system which depends entirely on inertial measurements for navigation. An INS consists of accelerometers which measure the translator acceleration and gyroscopes which measure the angular rotation of the system. This sensor array is called an Inertial Measurement Unit (IMU). This system can be equipped with camera to fine tuning and improve the inertial navigation near the target of interest. Radar systems are important sensors due to their all weather, day/night, long standoff capability. Along with the development of radar technologies, as well as with increasing demands for target identification in radar applications, automatic target recognition (ATR) using synthetic aperture radar (SAR) has become an active research area. Several researches introduced the template matching in recognizing and identifying objects [1-3]. Therefore, a large amount of works are limited to detecting and matching objects in synthesized shape databases [4-5] or in special image domains. Previous works [6-10] on template-based object detection extract low-level image features such as edges, corners, regions and interest points, and then locate the target boundary by grouping the features and matching them to

those on the template. Yijun Sun, et. al [11]. proposes a novel automatic target recognition (ATR) system for classification of three types of ground vehicles in the MSTAR public release database using SAR. Clark F. et. al [12]. perform automatic target recognition by matching sets of oriented edge pixels. A generalization of the Hausdorff measure that allows the determination of good matches between an oriented model edge map and an oriented image edge map was first proposed. Tuba[13], introduced an automatic target recognition in infrared imagery. Several researches introduce the simulation of SAR with Matlab program between them [14-17]. This paper introduce a simple template match object recognition technique able to detect and recognize the ground objects in the stage of fine tuning the INS for flying vehicles. SAR is a type of imaging radar in which the relative movement of the antenna with respect to the target is utilized. Through the simultaneous processing of the radar reflections over the movement of the antenna via the Range Doppler Algorithm (RDA). The results show superiority of this method for identifying and recognizing the ground objects.

II. THEORETICAL DESCRIPTION

Template matching is conceptually a simple process. We need to match a template to an image where the template is a sub-image that contains the shape we are trying to find. Accordingly, we centre the template on an image point and count up how many points in the template matched those in the image. The procedure is repeated for the entire image, and the point that led to best match, the maximum count, is defined to be the point where the shape (given by the template) lie within the image. If standard deviation of the template image compared to the source image is small enough, template matching may be used. Templates are most often used to identify printed characters, numbers, and other small, simple objects. Template matching is performed on either bi-level image (black and white) or grey level image depends on the application. For example, for character recognition and number plate of vehicle bi-level image are used while for vehicle recognition grey level image is used.

Formally, template matching can be defined as a method of parameter estimation. The parameters define the position of the template. We can define a template as a discrete function of T_{xy} . Template matching uses a similarity criterion for locating an object, where one common method calculates a correlation coefficient using the following equation [18],

$$p = \frac{\sum_x \sum_y (A_{xy} - \bar{A})(B_{xy} - \bar{B})}{\sqrt{(\sum_x \sum_y (A_{xy} - \bar{A})^2)(\sum_x \sum_y (B_{xy} - \bar{B})^2)}} \quad (1)$$

where A and B are image matrices, \bar{A} and \bar{B} are the 2-dimensional means of the respective image matrices, and

Manuscript received October 14, 2011, revised October 19, 2011.

Alaa El-Din Sayed Hafez is with Electrical engineering Department, Alexandria University, Alexandria, Egypt (email: alaahefaz@ieee.org).

Wiedo Hu is with Beijing University of Aeronautics & Astronautics, China (e-mail: weiduo.hu@gmail.com).

Ahmed Mohamed Gharyb is with Beijing University of Aeronautics & Astronautics, Egypt (email: ahmedgharyb@gmail.com).

(x,y) are the spatial coordinates within A and B. This correlation coefficient closely resembles a traditional statistical correlation, with the difference being that the traditional method is calculated in one dimension instead of two dimensions. A high correlation coefficient in a pixel-by-pixel comparison between the template and the region of interest (ROI) indicates a good match. This “cross-correlation” yields a result only if the integral is computed over the whole area g. The basic idea behind the hit-or-miss transform is that of extracting all pixels within an image that are matched by a given neighborhood configuration, consisting of some arrangement of foreground pixels and back-ground pixels. The neighborhood configuration is therefore defined by a pair of disjoint sets: one for the foreground pixels and the other for the background pixels. This can be represented mathematically as:

$$A \otimes B = \{p | B_{fgd} \subseteq A, B_{bgd} \subseteq A^c\} \quad (2)$$

where A is the image set, A^c is the complement of the image set, and B is the structure element. The algorithm flow chart is shown in Fig. 2. Fixed templates are useful when object shapes do not change with respect to the viewing angle of the camera. Two major techniques have been used in fix template matching, image subtraction and correlation. In the first technique, the template position is determined from minimizing the distance function between the template and various positions in the image. Although image subtraction techniques require less computation time than the following correlation techniques, they perform well in restricted environments where imaging conditions, such as image intensity and viewing angles between the template and images containing this template are the same. Matching by correlation utilizes the position of the normalized cross-correlation peak between a template and an image to locate the best match. This technique is generally immune to noise and illumination effects in the images, but suffers from high computational complexity caused by summations over the entire template. Point correlation can reduce the computational complexity to a small set of carefully chosen points for the summations. Dilation is one of the two basic operators in the area of mathematical morphology, the other being erosion. It is typically applied to binary images, but there are versions that work on grayscale images. The basic effect of the operator on a binary image is to gradually enlarge the boundaries of regions of foreground pixels (*i.e.* white pixels, typically) as shown in Fig. 2. Thus areas of foreground pixels grow in size while holes within those regions become smaller. The dilation operator takes two pieces of data as inputs. The first is the image which is to be dilated. The second is a (usually small) set of coordinate points known as a structuring element (also known as a kernel). It is this structuring element that determines the precise effect of the dilation on the input image. To compute the dilation of a binary input image by this structuring element, we consider each of the *background* pixels in the input image in turn.

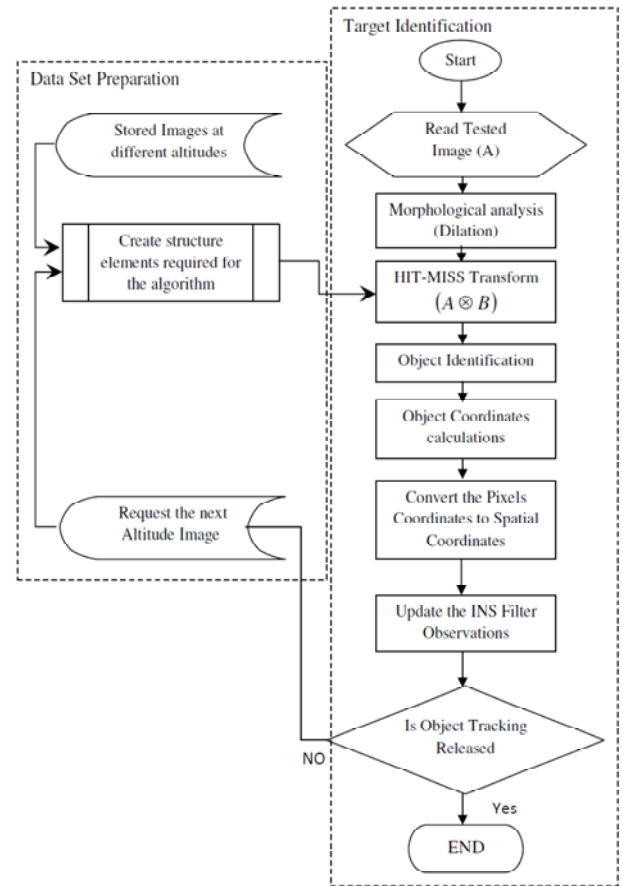


Fig. 1. Example of Template matching

For each background pixel (which we will call the *input pixel*) we superimpose the structuring element on top of the input image so that the origin of the structuring element coincides with the input pixel position. If *at least one* pixel in the structuring element coincides with a foreground pixel in the image underneath, then the input pixel is set to the foreground value. If all the corresponding pixels in the image are background, however, the input pixel is left at the background value.



Fig. 2. Dilation, Grow or Expand effect

A. Transmitted SAR signal

The transmitted radar signal, $S_{tx}(t)$, is assumed to be of the form in Equation (3) below in the simulation. The signal is a function of range time or quick time, t . Other important parameters are the signal bandwidth, B_0 in Equation (4) below, which is 100 MHz and the range resolution, ρ_r in Equation 3 below, which is approximately 1.5 m [19].

$$S_{tx}(t) = \text{rect}\left(\frac{t}{T_r}\right) \cos\{2\pi f_o + \pi K_r t^2\} = w_r(t) \cos\{2\pi f_o + \pi K_r t^2\} \quad (3)$$

$$B_o = |K_r| T_r \quad (4)$$

$$\rho_r \approx \frac{c}{2|K_r|T_r} = \frac{c}{2B_o} \quad (5)$$

The transmitted radar signal depicted as a cosine with a linearly ramping up frequency over a transmit duration followed by a null receive duration. The transmit window is called the pulse envelope, w_r , and defines the duration of the transmission. During the receive duration, the antenna waits to receive reflected radar signals from the targets contained in a one-dimensional range slice echo as function of quick time [20].

B. Received SAR Signal

The raw SAR received radar signal, $S_{rx}(t, \eta)$ for the simulation is assumed to be of the form shown in Equation (6) after quadrature demodulation which removes the high frequency carrier wave and brings the signal to baseband. Equation (6) is shown below as a summation of the reflections from M different point targets [20-21].

$$S_{rx}(t, \eta) = \sum_{m=0}^{M-1} \left[F_m w_r \left(t - \frac{2R_m(\eta)}{c} \right) w_a \left(\eta - \eta_c - i4\pi f_o R_m \eta c + i\pi K_r t - 2R_m \eta c + \eta m t, \eta \right) \right] \quad (6)$$

$$S_{rx}(t, \eta) = \sum_{m=0}^{M-1} \left[F_m w_r \left(t - \frac{2R_m(\eta)}{c} \right) w_a \left(\eta - \eta_c \right) \cos \left[2\pi f_o \left(t - R_m \eta c + \pi K_r t - 2R_m \eta c + \psi + \eta m t, \eta \right) \right] \right] \quad (7)$$

The time delay is $2R_m(\eta)/c$, the attenuation factor from reflection at the target is F_m , the phase shift from reflection at the target is ψ , the azimuth beam pattern amplitude modification is $w_a(\eta - \eta_c)$ as shown in Equation (8), and the additive white Gaussian noise is $n_m(t, \eta)$. The time delay is calculated by the distance the radar beam travels, twice the instantaneous slant range as shown in Equation (9), divided by the speed of the radar beam, approximately the speed of light. The attenuation factor, F_m , is a scalar value from 0 to 1 representing the normalized reflectivity of each point target. Phase shift information, ψ , is not used in the simulation. The azimuth beam pattern amplitude modification, $w_a(\eta - \eta_c)$, is named due to the geometrical shape of the beam pattern in the azimuth plane as shown in Fig. 3. The center node of the beam pattern produces the largest reflection strength, but the smaller side nodes also produce reflections and the overall received signal strength from a point target over azimuth time, η , resembles a sinc squared function centered at the beam center crossing time η_c , which is the azimuth time at which the center of the beam pattern crosses the center target area. The azimuth beam width, β_{bw} used in Equation (8) for calculation of the azimuth beam pattern, is calculated in Equation 10 and is inversely proportional to the actual antenna length, L_a .

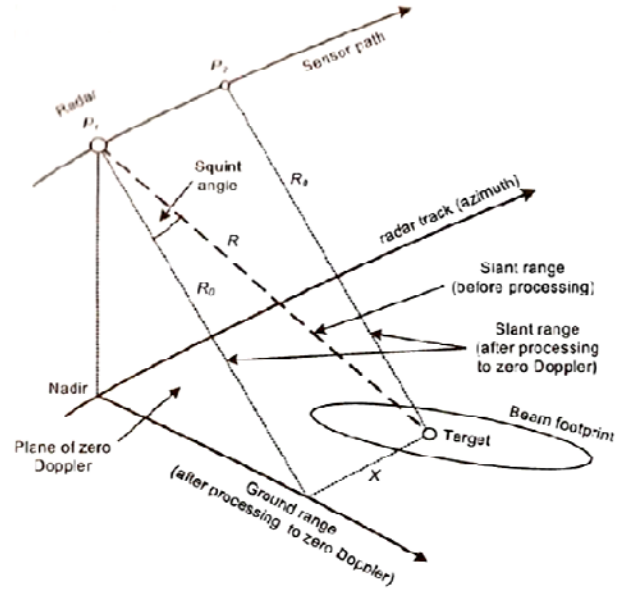


Fig. 3: SAR slant range and squint angle geometry

$$w_a(\eta) \approx \text{sinc}^2 \left(\frac{0.886\theta(\eta)}{\beta_{bw}} \right) \quad (8)$$

$$R_m(\eta) = \sqrt{R_{om}^2 + V_r^2 \eta^2} = \sqrt{(X_o - x_m)^2 + V_p^2 \left(\eta + \frac{y_m}{V_p} \right)^2} \quad (9)$$

$$\beta_{bw} = 0.866\lambda/L_a \quad (10)$$

Important in understanding the effectiveness of SAR processing is the azimuth resolution, ρ_a , as show in Equation(11) below. Simplifications and approximations due to the airplane platform as opposed to satellite in the simulation lead to the approximation of the azimuth resolution to be $L_a/2$. The antenna length parameter in the MATLAB simulation is set to 2 m, leading to an azimuth resolution of 1 m, which is superior to the range resolution of 1.5 m. The azimuth resolution is first shown before simplification as a function of radar beam ground velocity, v_g , squint angle, θ_{sq} , azimuth bandwidth, and Δf_{dop} . The Doppler bandwidth equation is shown in Equation (12) as a function of the orbital velocity, squint angle, wavelength, and 3 dB azimuth width of the main lobe of the azimuth radar beam shown in Fig. 6.

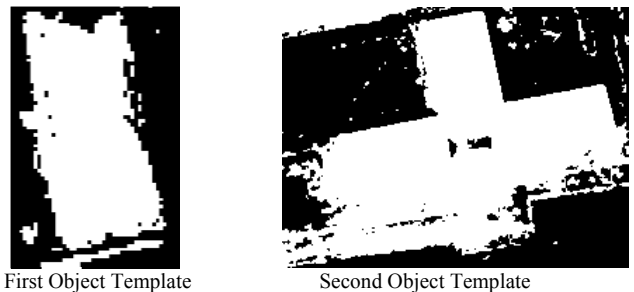


Fig. 6. The Two Objects Templates

$$\rho_a = \frac{0.866V_g \cos\theta_{sq}}{\Delta f_{dop}} = \frac{L_a}{2} \quad (11)$$

$$\Delta f_{dop} = \frac{2V_s \cos\theta_{sq}}{\lambda} \theta_{bw} \quad (12)$$

Squint angle, θ_{sq} , used in Equations (11) and (12), is

labeled below in Fig. 3 as the angle between the slant range vector and the zero Doppler plane. Squint angle varies as a function of slow time, η , decreasing as the platform approaches the target and increasing as the platform moves away from the target as shown in Equation (13) below. The maximum squint angle, θ_{sqmax} , calculation is shown in Equation (14) below and for the MATLAB simulation is 0.859° , which is low due to the simulation flight duration of 3 seconds.

$$\theta_{sq} = \arccos\left(\frac{R_{om}}{R_m(\eta)}\right) \quad (13)$$

$$\theta_{sqmax} = \arccos\left(\frac{R_{om}}{R_m(\eta)}\right)\Big|_{R_m(\eta)=\left(\frac{dur}{2}\right)v_p} = \arccos\left(\frac{2R_{om}}{dur v_p}\right) \quad (14)$$

III. SIMULATION RESULTS

The proposed method is simulated using Matlab program and the numerical experiments are shown to verify the object detection for a wide range altitude and orientation. The test image used is a satellite image includes two target objects. These targets are shown in Fig. 4. The identification mechanism is tested at five altitudes, 8034, 7632, 7230, 7084, and 6888 feet respectively. The satellite images at different altitudes are shown in Fig. 5. Each altitude is tested at different approaching angles, 0, 90, 180, 270 degree respectively. The generated templates for the two object after the hit/miss transform is shown in Fig. 6. Fig. 7. to 9. demonstrate the object (1) and object (2) identification and detection at different altitudes and orientation angles. The algorithm is evaluated on twelve different altitudes for two Objects. Fig. 10. shows that the first object miss detection below 18% and false alarm detection below 6 %. The second object with relatively large area satisfies results better than the first object which satisfies miss detection below 12% and false alarm detection below 4% as shown in Fig. 11.



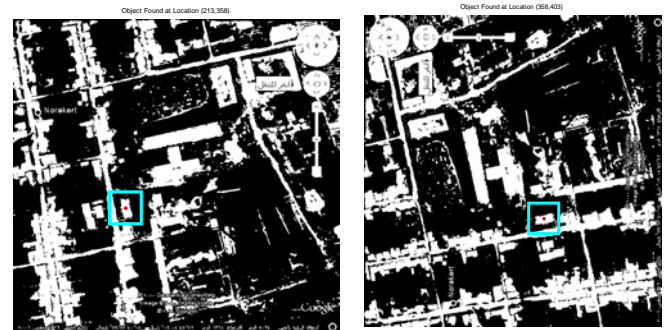
7084 feet

6888 feet

Fig. 5. The satellite image at different altitudes

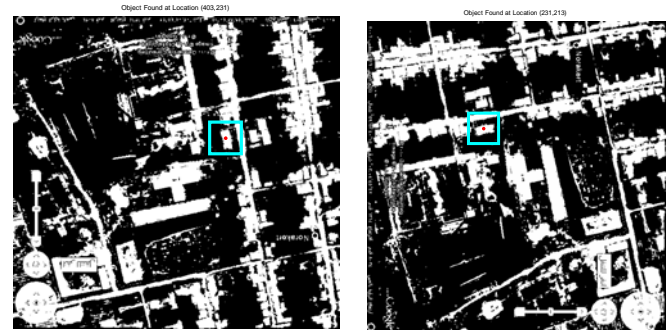


Fig. 4. The satellite test image include the two targets



0 Degree Orientation

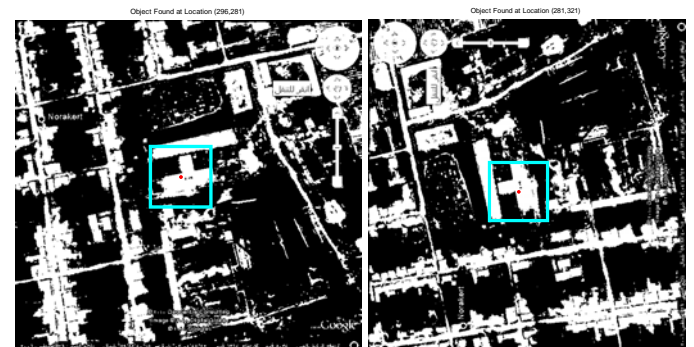
90 Degree Orientation



180 Degree Orientation

270 Degree Orientation

Fig. 7. Object (1) detection at 8034 feet altitude



0 Degree Orientation

90 Degree Orientation

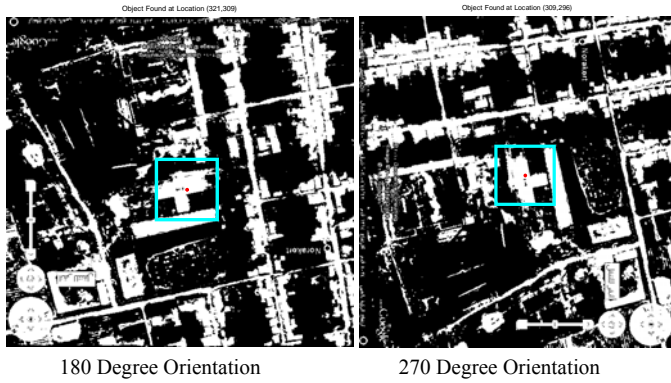


Fig. 8. Object (2) detection at 8034 feet altitude

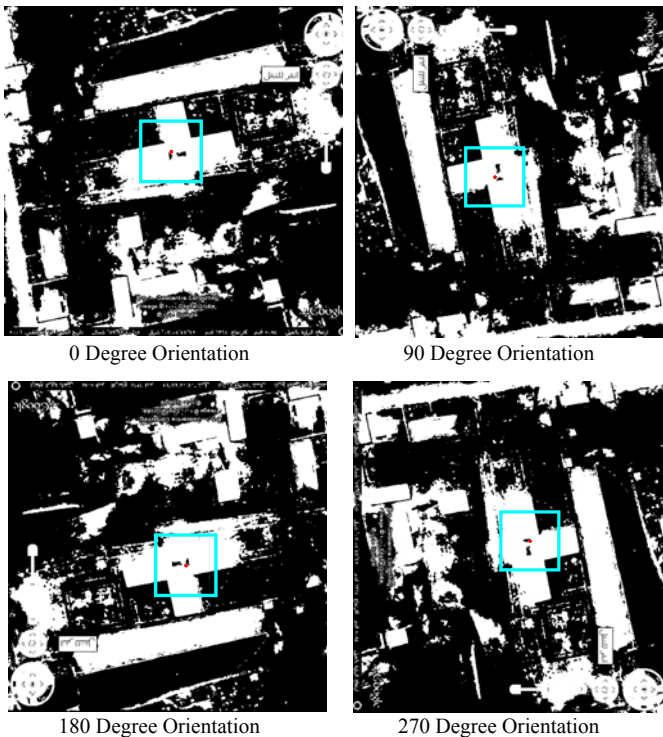


Fig. 9. Object (2) detection at 7084 feet altitude

The simulated SAR with PRF 300 Hz and the simulation duration is 3 seconds. This equates to 900 transmitted radar pulses over the duration of the simulation. The result of the plot of the magnitude of each range slice echo as a function of range and azimuth is the raw SAR signal space. The antenna length parameter in the MATLAB simulation is set to 2 m, leading to an azimuth resolution of 1 m, which is superior to the range resolution of 1.5 m. The carrier frequency, f_0 , is 4.5 GHz. The chirp pulse duration, T_r , is 2.5 μ s and the range chirp or FM rate, K_r , is +40 MHz/ μ s, which is called an up-chirp because it is positive. The extracted features from 5000 to 8034 feet SAR image is shown in Figs. 12 to 17. SAR extracts the ground target edges that will be required for recognizing it from SAR images during the bad weather conditions. Predefined SAR images of the ground target are stored in the recognizing library. The received SAR images are correlated with the predefined images, the recognized images maximizes the output of the recognition system. The simulation results show that SAR is able to detect and

recognize the ground targets in bad weather conditions.

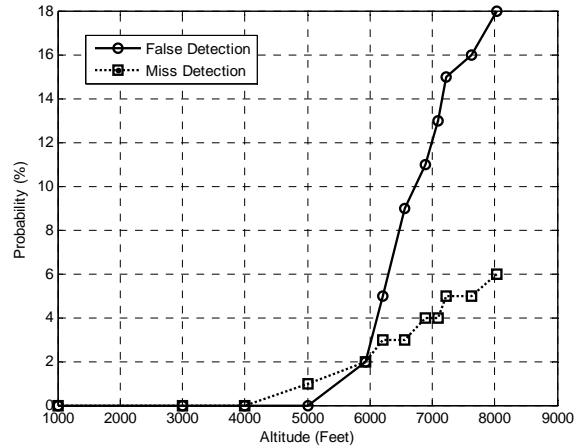


Fig. 10. Object (1) detection at different altitudes

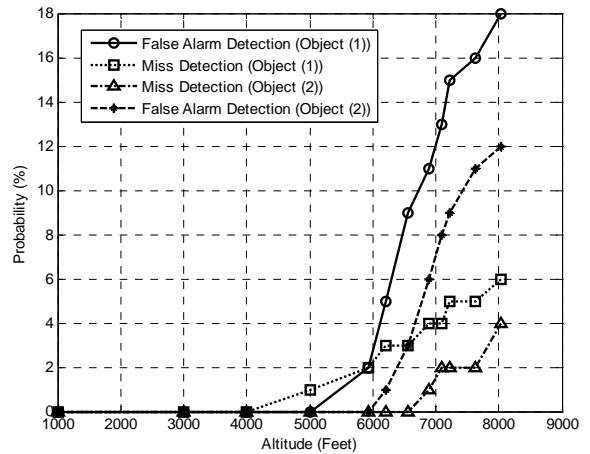
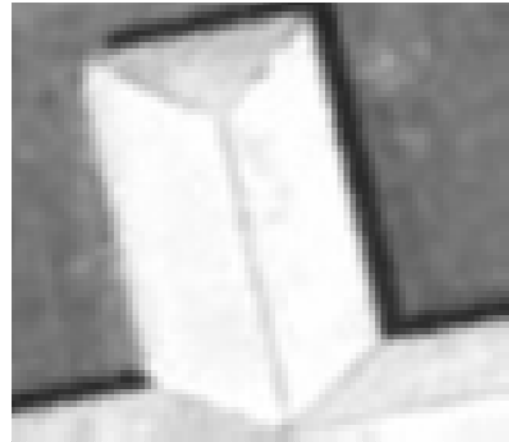
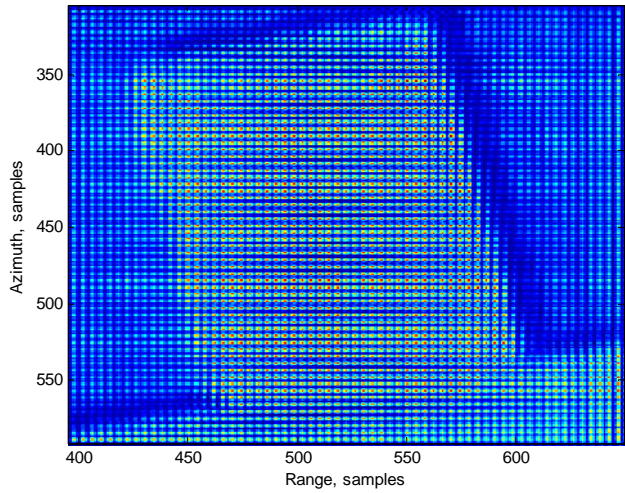


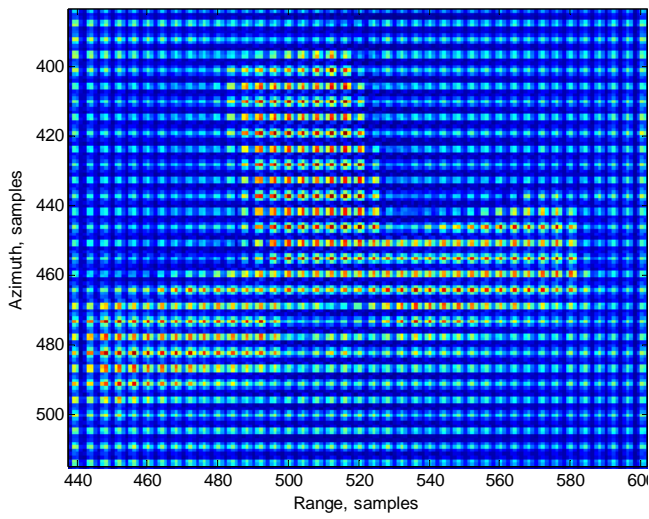
Fig. 11. Object (2) detection at different altitudes compared with Object (1)

IV. CONCLUSION

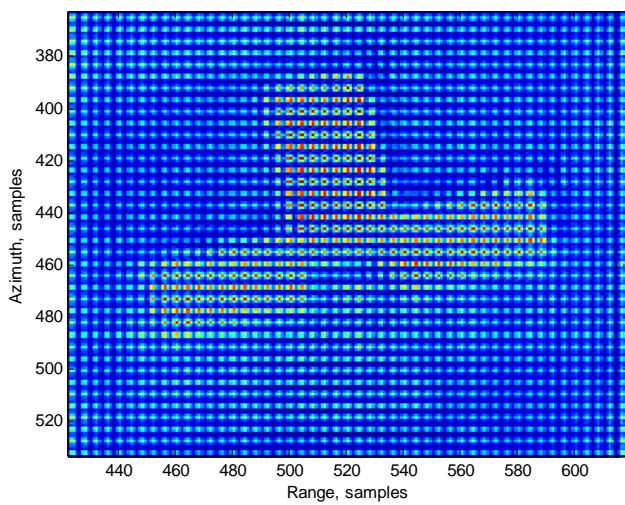
This paper introduces a simple template match object recognition technique able to detect and recognize the ground objects in the stage of fine tuning the INS for flying vehicles. The proposed method is an image processing technique to improve the precision of the INS for detecting and tracking the ground objects. Template matching technique is one of the methods used for ground object detection and tracking. The paper focus is on flying systems equipped with camera to capture photos for the ground and recognize it. Automatic Target Recognition (ATR) using SAR images for inertial navigation systems (INS) is also proposed. This improves the precision of the INS for detecting and tracking the ground objects from flying vehicles. Synthetic Aperture Radar (SAR) is used as ground object detection with ATR technique. The algorithm is simulated using Matlab program and the numerical simulation are shown which verify the object detection for a wide range altitude. The results show superiority of this method for identifying and recognizing the ground objects. The proposed method is independent on the altitude or the orientation of the object. The system successfully recognized and detects the ground objects at different altitudes and orientation.



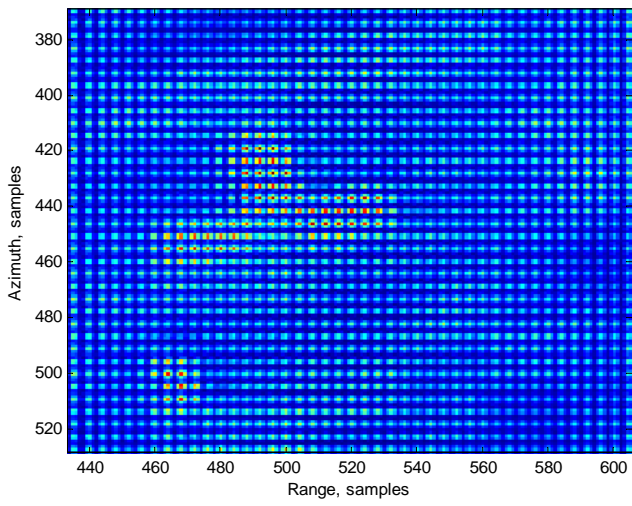
(a) (b)
Fig. 12. Object (2) SAR detection at 5000 feet altitude, (a) The formed SAR image (b) The photographic Image



(a) (b)
Fig. 13. Object (2) SAR detection at 6888 feet altitude, (a) The formed SAR image (b) The photographic Image



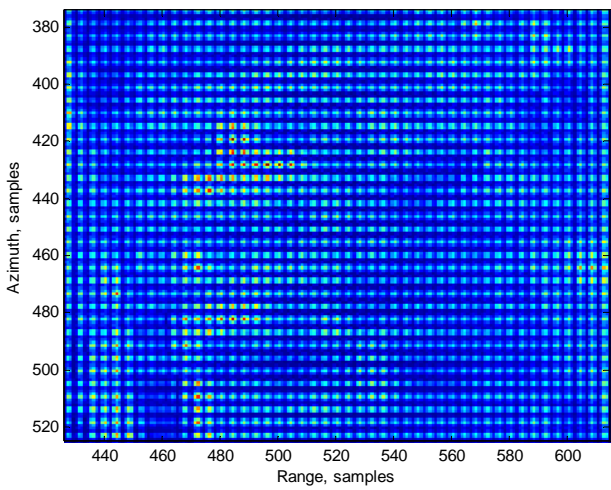
(a) (b)
Fig. 14. Object (2) SAR detection at 7084 feet altitude, (a) The formed SAR image (b) The photographic Image



(a)

(b)

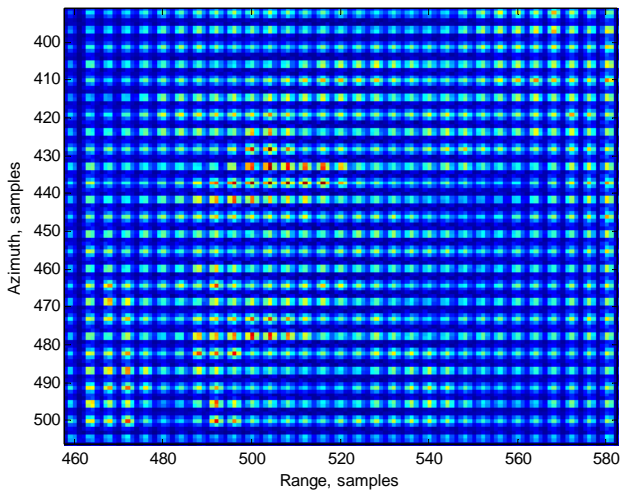
Fig. 15. Object (2) SAR detection at 7230 feet altitude, (a) The formed SAR image (b) The photographic Image



(a)

(b)

Fig. 16. Object (2) SAR detection at 7632 feet altitude, (a) The formed SAR image (b) The photographic Image



(a)

(b)

Fig. 17. Object (2) SAR detection at 8034 feet altitude, (a) The formed SAR image (b) The photographic Image

REFERENCES

- [1] Roger M. Dufour, Eric L. Miller, and Nikolas P. Galatsanos, "Template Matching Based Object Recognition With Unknown Geometric Parameters," *IEEE Transaction on Image Processing*, VOL. 11, NO. 12, Dec. 2002.
- [2] Gupta, Rahul Gupta, Amardeep Singh, Matt Wytock, "Object Recognition using Template Matching," Stamford University <http://www.stanford.edu/class/cs229/proj2008>.
- [3] R. Brunelli, *Template Matching Techniques in Computer Vision: Theory and Practice*, Wiley, ISBN 978-0-470-51706-2, 2009
- [4] Kyriacou, Theocharis, Guido Bugmann, and Stanislaw Lauria, "Vision-based urban navigation procedures for verbally instructed robots" *Robotics and Autonomous Systems*, Expanded Academic ASAP No. 30, 2005.
- [5] Zhao Yu-qian^{1, 2}, Gui Wei-hua², Chen Zhen-cheng¹, Tang Jing-tian¹, Li Ling-yun¹, "Medical Images Edge Detection Based on Mathematical Morphology," *Proceedings of IEEE Engineering in Medicine and Biology 27th Annual Conference Shanghai, China*, September 1-4, 2005.
- [6] Li, Y.; Tsin, Y.; Genc, Y.; Kanade, T., "Object detection using 2D spatial ordering constraints," *Computer Vision and Pattern Recognition, CVPR 2005. IEEE Computer Society Conference on*, 20-25 June 2005.
- [7] Heisele, B.; Rocha, C., "Local shape features for object recognition," *Pattern Recognition, 2008. ICPR 2008 19th International Conference on*, Tampa, FL, 8-11 Dec. 2008
- [8] Neal R. Harvey, Reid Porter, and James Theiler, "Ship detection in satellite imagery using rank-order grayscale hit-or-miss transforms," *Proc. SPIE*, Vol. **7701**, 2010.
- [9] E. G. M. Petrakis, A. Diplaros, and E. Miliou, "Matching and retrieval of distorted and occluded shapes using dynamic programming," *IEEE Transactions on Pattern Analysis and Machine Intelligence* Vol. 24 No. 11, 2002.
- [10] Feng Ge, Tiecheng Liu, Song Wang, Joachim Stahl, "Template-Based Object Detection through Partial Shape Matching and Boundary Verification," *International Journal of Information and Communication Engineering* Vol.4 No. 2, 2008.
- [11] Yijun Sun, Zhipeng Liu, Sinisa Todorovic, and Jian Li, "Synthetic Aperture Radar Automatic Target Recognition Using Adaptive Boosting," *Proceedings of the SPIE*, Volume 5808, pp. 282-293 (2005)
- [12] Clark F. Olson and Daniel P. Huttenlocher, "Automatic Target Recognition by Matching Oriented Edge Pixels," *IEEE Transaction on Image Processing*, Vol. 6, No. 1, Jan. 1997.
- [13] Tuba Makbule Bayik, "Automatic Target Recognition in infrared," *Ms.c. Graduate School Of Natural and Applied Sciences*, Middle East Technical University, 2004.
- [14] David Sandwell, "SAR Image Formation: ERS SAR Processor coded in Matlab," *Polar conference*, 2010.
- [15] Grant D. Martin, Armin W. Doerry, "SAR Polar Format Implementation with Matlab," *Sandia National Laboratories*, 2005.
- [16] Mireia Cequiel Mir, "Image formation for Synthetic Aperture Radar using MATLAB," *institute of higher education, NEWI*, 2000.
- [17] Matthew Schlutz, "Synthetic Aperture Radar Imaging Simulated in MATLAB," *Ms.c. Faculty of the California Polytechnic State University, San Luis Obispo*, 2009.
- [18] Rjiv Kumar Nathi, "On Road Vehicle/Object Detection Template," *Indian Computer and Science and Engineering* Vol. 1 No. 2, 2010.
- [19] Merrill Skolnik, "Radar Handbook," *McGraw-Hill*, New York, 1990.
- [20] Nadav Levanon, "RADAR SIGNALS," *A John Wiley & Sons*, Canada, 2004.
- [21] David K. Barton Sergey A. Leonov, "Radar Technology Encyclopedia," *Artch House, INC*, Norwood, 1998.



Alaa El-Din Sayed Hafez is an affiliate instructor in Faculty of Engineering, Alexandria University, Alexandria, Egypt. He holds B.Sc. in Electronics and Communications from Faculty of Engineering, Alexandria University, M.Sc. in Electronics and Communication from Arab Academy for Science and Technology and Maritime Transport, Alexandria. He also holds M.Sc. and Ph.D. in Electrical Engineering from Faculty of Engineering, Alexandria University.

He received many technical courses in Surveillance Radar design and Implementation, work as Radar System Engineer for more than 5 years, teach up to 20 undergraduate subjects, supervising more than 12 thesis, publish more than 40 papers in different international conferences and journals.

Weiduo Hu, Professor, Dept. of Aerospace Engineering, BeiHang University, Beijing, Chin. He got his Bachelor degree from Beijing University of Aeronautics and Astronautics. He worked as a senior engineer in Beijing Institute of Control Engineering, dealing with satellite control system design and simulation. Ph.D. form Department of Aerospace Engineering at the University of Michigan.

Ahmed Mohamed Gharyb is Ph.D. student in Beijing University of Aeronautics and Astronautics, He holds B.Sc. in Electronics and Communications from Faculty of Engineering, Alexandria University, M.Sc. in Electrical Engineering from Faculty of Engineering, Alexandria University.